Mass spectrometric analysis of lipid-linked oligosaccharide heterogeneity in genetically modified E. coli used for glycoconjugate bacterial vaccine production

Palubeckaite, I.; Moran, A.B.; Cramer, D.A.T.; Torrente López, A.; Smits, W.K.; Weerdenburg, E.; ... ; Nicolardi, S.

Carbohydrate Polymers 366 (2025) 123928

Contents lists available at ScienceDirect

Carbohydrate Polymers

journal homepage: www.elsevier.com/locate/carbpol

Mass spectrometric analysis of lipid-linked oligosaccharide heterogeneity in genetically modified *E. coli* used for glycoconjugate bacterial vaccine production

Ieva Palubeckaite [a], Alan B. Moran [b], Dario A.T. Cramer [a], Anabel Torrente-López [a], Wiep Klaas Smits [c], Eveline Weerdenburg [b], Ali Al Kaabi [d], Michel Beurret [b], Chakkumkal Anish [b,1], Manfred Wuhrer [a], Simone Nicolardi [a,*]

[a] Center for Proteomics and Metabolomics, Leiden University Medical Center, Albinusdreef 2, 2333 ZA Leiden, the Netherlands
[b] Bacterial Vaccines Discovery and Early Development, Janssen Vaccines & Prevention B.V., Archimedesweg 4-6, 2333 CN Leiden, the Netherlands
[c] Experimental Bacteriology group, Leiden University Center for Infectious Diseases, Leiden University Medical Center, Albinusdreef 2, 2333 ZA Leiden, the Netherlands
[d] Janssen Vaccines AG (Branch of Cilag GmbH International), Rehhagstrasse 79, CH-3018 Bern, Switzerland

A B S T R A C T

Polysaccharide-based glycoconjugate bacterial vaccines can help combat multidrug-resistant pathogens by harnessing the immune system to recognize and neutralize bacteria effectively. Bacterial cells can be engineered to link O-antigen polysaccharides (O-PSs) to a carrier protein, producing a potential bacterial vaccine, e.g., against extraintestinal pathogenic *Escherichia coli* (ExPEC). Lipid-linked oligosaccharides (LLOs) play a key role in the bioconjugation process, and determining their heterogeneity is essential to evaluate the variability among clinical isolates and the success of the bioengineering process. Mass spectrometry (MS) techniques can provide unique structural insights, but applications have typically been limited to short LLOs or hydrolyzed LLO fragments.

Here, we used ultrahigh-resolution MALDI MS to analyze LLOs from an engineered *E. coli* strain expressing *E. coli* O2 O-PSs. Two methods were evaluated: (1) analysis of LLOs after extraction and purification, and (2) analysis of hydrolyzed O-PS fragments obtained by mild acidic hydrolysis of bacterial biomass. Negative and positive ion mode measurements revealed LLO structural polydispersity and heterogeneity, while MS/MS confirmed RU monosaccharide composition and structural consistency with glycoconjugate-derived O-antigens. The hydrolysis-based approach also enabled rapid RU profiling with some limitations. This study highlights MALDI FT-ICR MS as an effective tool for analyzing bacterial LLOs and advancing ExPEC-targeted glycoconjugate vaccines.

Hypothesis statement: We hypothesize that ultrahigh-resolution MALDI FT-ICR mass spectrometry can reliably characterize the structural heterogeneity and repeat unit composition of lipid-linked oligosaccharides (LLOs) from engineered *E. coli* strains, thereby providing critical analytical insights to support the development of glycoconjugate vaccines against extraintestinal pathogenic *E. coli* (ExPEC).

1. Introduction

The rise of multidrug resistance is straining healthcare systems globally, underscoring the urgent need for effective bacterial vaccines (Frost et al., 2023; Hernandez-Pastor et al., 2023; Ikuta et al., 2022; MacKinnon et al., 2021; Naghavi et al., 2024; Poolman & Wacker, 2015).

Escherichia coli (*E. coli*), a commensal Gram-negative bacterium, is capable of causing both intestinal and extraintestinal infections (Kaper et al., 2004; Manges et al., 2019). Strains belonging to certain pathotypes, such as extraintestinal pathogenic *E. coli* (ExPEC), are significant pathogens, being the primary cause of urinary tract infections (UTIs) and bacteremia (Poolman & Wacker, 2015; Weerdenburg et al., 2022). Traditionally, *E. coli* has been classified phenotypically based on surface antigens, including O-polysaccharides (O-PSs), H-antigens, and K-antigens (Fratamico et al., 2016). O-PSs are components of the lipopolysaccharide (LPS) molecules on the outer membrane of Gram-negative bacteria (Liu et al., 2019). Almost 190 distinct O-antigen structures have been identified in *E. coli*, differing in monosaccharide composition, glycosidic linkages, anomeric configuration, and modifications. Among ExPEC strains, O25, O2, O6, O1, and O75 are the most prevalent serotypes in bloodstream infections on a global level (Liu et al., 2019; Weerdenburg et al., 2022).

Various vaccine strategies have been explored to produce an effective vaccine against ExPEC, including live-attenuated cells, lysate fractions, heat-inactivated whole cells, protein subunits, and polysaccharide

* Corresponding author.
E-mail address: s.nicolardi@lumc.nl (S. Nicolardi).
[1] Present address: Vaccine & Immunotherapies Division, AstraZeneca, 1 Medimmune Way, Gaithersburg, MD 20878, USA.

https://doi.org/10.1016/j.carbpol.2025.123928
Received 19 April 2025; Received in revised form 13 June 2025; Accepted 18 June 2025
Available online 19 June 2025

conjugates, however, no vaccine has been licensed for human use (Qiu et al., 2024). Since O-PSs are key molecular targets recognized by the host immune system, a potential strategy for creating bacterial vaccines involves bioconjugating O-PSs to an immunogenic carrier protein that induces a durable and strong T-cell dependent PS-specific immune response, known to be protective against invasive diseases (Feldman et al., 2005; Fierro et al., 2023; Huttner et al., 2017; Reeves, 1995; van den Dobbelsteen et al., 2016; Wantuch et al., 2024; Whitfield et al., 2020). Bioconjugation is achieved by engineering microbial cells, such as recombinant *E. coli*, to express the enzymes for O-PSs biosynthesis, a carrier protein, and a specific oligosaccharyltransferase that links the two together in the periplasmic space, creating efficient bacterial vaccine factories (Feldman et al., 2005). The O-PS precursor molecules for such a bioconjugation – the lipid-linked oligosaccharides (LLOs) – contain polydisperse polysaccharide chains consisting of repeat units (RUs) that may exhibit structural heterogeneity due to variations in the glycan composition and the presence of modifications (Fig. 1) (Liu et al., 2019).

Three major O-PS synthesis pathways have been proposed for Gram-negative bacteria, namely the Wzy-dependent, the ABC-transporter-dependent and the synthase-dependent pathways (Raetz & Whitfield, 2002; Woodward et al., 2010). These start in the cytoplasm with the linkage of a first monosaccharide to undecaprenyl pyrophosphate and the subsequent formation of the RU structure. Most of the heteropolymeric O-antigens are synthesized via the Wzy-dependent pathway, in which the lipid-linked single RUs are translocated to the periplasm where they are polymerized by the joint action of both the Wzy and Wzz proteins with the latter acting as an O-antigen chain length regulator (Woodward et al., 2010). In wild-type *E. coli* strains, O-PSs are transferred from LLOs to lipid A-core oligosaccharide (core-lipid A) molecules by the WaaL ligase, resulting in the formation of LPS. These LPS molecules are then transported to the outer membrane via the Lpt system. In genetically modified *E. coli* strains engineered for glycoconjugate vaccine production, deletion of the WaaL gene will abrogate the LPS biosynthesis pathway and make LLOs available for bioconjugation. As a result, these strains display rough LPS on their outer surface, lacking the full O-antigen structure. Instead, the expression of an oligosaccharyltransferase enzyme such as PglB from *Campylobacter jejuni* allows the conjugation of the O-PS to the carrier protein (Dow et al., 2020; Kowarik et al., 2021).

A detailed structural understanding of LLOs is critical for evaluating glycoengineering success and ensuring structural consistency of lipid-linked O-PS with protein-conjugated O-PS (Di Marco et al., 2024). Mass spectrometry (MS) provides detailed structural information with minimal sample requirements (Alley Jr. et al., 2013; Harvey, 2025). In the literature, examples of MS applications for the analysis of bacterial LLOs at intact levels are scarce. Reid and coworkers reported on the use of capillary electrophoresis MS and porous graphitic carbon liquid chromatography MS for the analysis of LLOs from *Campylobacter jejuni* highlighting the heterogeneity of both the lipid and glycan moieties, with the glycan part being short, consisting of either five or six monosaccharides (Reid et al., 2008; Reid et al., 2009; Reid et al., 2010). Short *E. coli* LLOs (i.e. up to 2RUs) were analyzed after 2AB-derivatization and LC separation by MALDI MS/MS by Kowarik et al. (2021) and Wetter et al. (2013). However, *E. coli* can express longer O-antigens ranging from one to tens of RUs as deduced by the characteristic ladder pattern in gel-electrophoresis analysis of LPS of different serotypes (del Mar Tavío et al., 2000; Guo et al., 2005; Perry et al., 1986; Tirsoaga et al., 2007; Wang et al., 2023). A few reports described the MS-based analysis of long *E. coli* O-PSs present on LPS but not as LLO molecules (Pupo et al.,

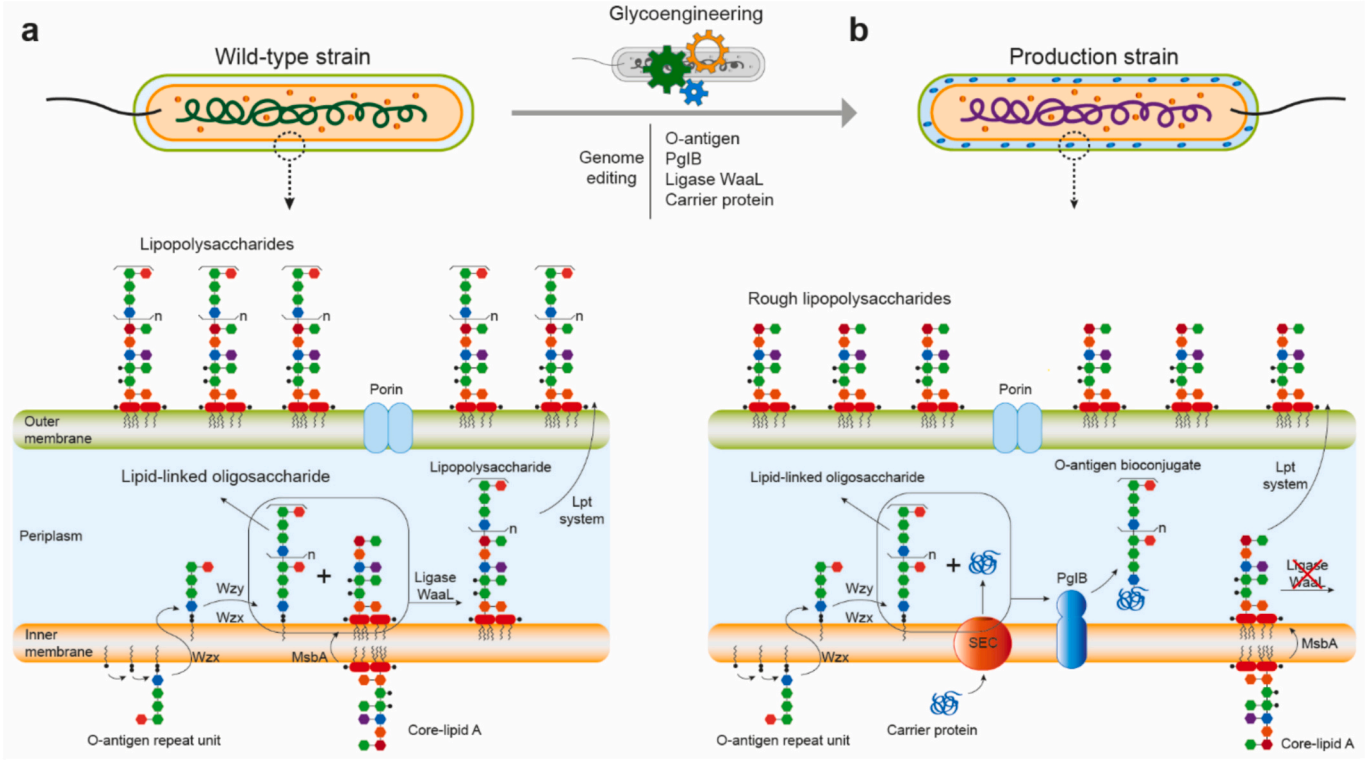

Fig. 1. a) Schematic representation of the LPS biosynthesis pathway in wild-type *E. coli* strains expressing heteroglycan O-antigens. In this pathway, individual heteroglycan O-antigen repeating units (RUs) are first generated in the cytoplasm, attached to an undecaprenyl pyrophosphate molecule. This lipid-linked glycan is then transported to the periplasm, where the RUs are assembled into lipid-linked oligosaccharides (LLOs). Mature O-polysaccharides (O-PSs) are subsequently transferred from the LLOs to the core-lipid A structure via the WaaL ligase. Finally, the complete LPS is exported to the outer membrane through the Lpt system. **b)** Schematic representation of O-antigen bioconjugate biosynthesis in glycoengineered *E. coli* strains. In these modified strains, LLOs are synthesized similarly to wild-type cells, but instead of being incorporated into LPS, mature O-PSs are transferred from the LLOs to a carrier protein by the PglB oligosaccharyltransferase, forming the O-antigen glycoconjugate vaccine. The deletion or mutation of the WaaL ligase gene prevents the assembly of LPS, resulting in a rough LPS structure.

2021; Tirsoaga et al., 2007).

In this study, we applied ultrahigh resolution matrix-assisted laser desorption/ionization (MALDI) Fourier-transform ion cyclotron resonance (FT-ICR) MS to analyze LLOs from an *E. coli* K-12 strain genetically modified to produce O2-type O-PS (i.e. →3)-[α-D-Fuc*p*3NAc-(1 → 2)]-α-L-Rha*p*-(1 → 2)-α-L-Rha*p*-(1 → 3)-β-L-Rha*p*-(1 → 4)-β-D-Glc*p*NAc-(1 → RU) (Jansson et al., 1987). We used a precursor strain containing a WaaL ligase gene mutation to block the expression of full-length LPS. This strain differs from the complete bioconjugation production strain that also contains the PgIB and the carrier protein plasmids. Two characterization strategies were employed: (1) after extraction and (partial) purification of LLOs and (2) after mild acidic hydrolysis performed on *E. coli* biomass adapted from what was recently proposed by Urakami and Hinou (2024). We show that the acquisition of isotopically resolved mass spectra in negative and positive ion modes, across an extensive mass-to-charge (*m/z*) range, enables the confident determination of LLO structural heterogeneity. Furthermore, we used MS/MS to corroborate the RU monosaccharide composition and prove the structural consistency with O-antigens present on a glycoconjugate protein obtained from a complete *E. coli* production strain and previously characterized by MALDI in-source decay (ISD) FT-ICR MS (Nicolardi et al., 2022). Finally, we show that the analysis of hydrolyzed LLOs provides fast access to RU information and describe some limitations of the method.

2. Experimental

2.1. E. coli strain

The biomass of a recombinant *E. coli* W3110 precursor strain genetically modified to produce *E. coli* O2 O-PSs was provided by Janssen Vaccines and Prevention B.V. (Leiden, the Netherlands) (Kowarik et al., 2021; Poolman & Wacker, 2015). This strain, containing a WaaL ligase mutation, was unable to produce full-length LPS allowing the enrichment of the LLOs. Such a precursor strain can be further engineered into a production strain by introducing PglB and carrier protein plasmids, enabling the biosynthesis of the polysaccharide-based glycoconjugate (Dow et al., 2020; Khlebnikov et al., 2000).

2.2. Bacterial culture

The recombinant *E. coli* production strain was cultured overnight at 37 °C on a lysogeny broth (LB) agar in a Petri dish. Then 100 mL (in a 500 mL flask) of LB was inoculated with a single colony from the LB agar plate and incubated for 18 h in a shaking incubator at 37 °C and 200 rpm. Then, *E. coli* cells were harvested by transferring the LB to 50 mL Falcon tubes and centrifuging for 10 min at 5500 ×*g* at 4 °C. After removing the medium, cells were inactivated by adding 10 mL of 70 % ice-cold ethanol to each tube. Thus, cells were resuspended by vortexing and incubated at room temperature for 5 min. The ethanol solution was removed after centrifugation for 10 min at 5500 ×*g* at 4 °C. The cells were then frozen at −20 °C and then lyophilized overnight.

2.3. LLOs extraction and purification

LLOs were extracted from 83 mg of *E. coli* lyophilized biomass as follows. In a 2 mL Eppendorf tube, the biomass was mixed with 0.250 mL of 0.1 mm and 0.250 mL of 0.5 mm glass beads, and 652 μL of water and was homogenized for 3 min in a homogenizer (Bullet Blender 24 at speed 8, Next Advance, USA). After 10 s of speed centrifugation, the liquid was transferred to a 7.5 mL glass tube together with 2.174 mL of methanol and 2.174 mL of chloroform. The tube was shaken for 40 min at 1300 rpm on a plate shaker (Titramax 100, Heidolph, Germany). After 10 min centrifugation at 4000 ×*g*, the supernatant was transferred to a 12 mL glass tube and 5 mL of a 10:10:3 (v/v/v) chloroform:methanol: water (CMW) solution were added to the residue. The tube with the residue was shaken for 10 min at 1300 rpm and then centrifuged again. The supernatant was combined in the 12 mL tube. The extract was dried under a stream of nitrogen at 45 °C, reconstituted in 5 mL of 3:48:47 (v/v/v) CMW solution, incubated for 2 min at 50 °C and centrifuged for 5 min at 3000 ×*g*. The LLO purification was performed using a tC18-SepPak SPE cartridge (500 mg/6 mL) using a rack of pressure processor. The extract was loaded onto a pre-equilibrated cartridge and washed with 5 mL of 3:48:47 (v/v/v) CMW solution. The LLOs were eluted with 5 mL of methanol which was then evaporated under a stream of nitrogen at 45 °C. The LLOs were reconstituted in 150 μL of methanol and kept at 8 °C until analysis.

2.4. Mild acidic hydrolysis of E. coli biomass

Mild acidic hydrolysis was performed directly on 5 mg of lyophilized *E. coli* biomass. Thus, the biomass was transferred to a 1 mL Eppendorf tube and washed twice with 1 mL of water by centrifuging at 10000 rpm for 2 min and discarding the supernatant. The washed biomass was mixed with 30 μL of water. 1 μL of the suspended biomass was transferred to a 100 μL tube and incubated with 49 μL of a 400 mM HCl solution for 10 min at 80 °C. After incubation, the sample was centrifuged at 14,000 rpm for 3.5 min at room temperature.

2.5. MALDI sample spotting

The purified LLO extract (1 μL) was spotted onto a polished-steel MALDI target plate (Bruker) and mixed with a 1 μL of a 2,5-dihydroxyacetophenone (DHAP) solution (i.e. 7.6 mg DHAP were suspended in 375 μL EtOH and 125 μL of an 80 mM diammonium hydrogen citrate solution). The spot was left to dry at room temperature. To enhance the formation of LLO ISD fragment ions, the LLO extract (1 μL) was spotted with 1 μL of an α-cyano-4-hydroxycinnamic acid (α-cyano) solution (saturated in 50:50 (*v*/v) acetonitrile:water). Hydrolyzed LLOs (0.5 μL) were spotted with a 2,5-dihydroxybenzoic acid (DHB), 1,5-diaminonaphtalene (1,5-DAN) and ammonium bicarbonate mixture (0.5 μL) prepared as previously reported by Urakami and Hinou: 2 μL of 500 mM DHB in acetonitrile/water (9:1, *v*/v), 4 μL of 50 mM 1,5-DAN in acetonitrile/ water (1:1, v/v), and 1 μL of 100 mM NaHCO3 in water were mixed and diluted to 100 μL in an acetonitrile/ water (1:1 v/v) solution (Urakami & Hinou, 2024). The sample and matrix mixture were spotted onto a polished-steel MALDI plate kept on a heater block set at 40 °C to accelerate evaporation.

2.6. MALDI-ISD FT-ICR mass spectrometry

MS measurements were performed on a 15 T solariX XR FT-ICR mass spectrometer (Bruker Daltonics, Bremen, Germany) equipped with a CombiSource and a ParaCell (2xR). The MS system was operated in 1 omega mode using ftmsControl software (Bruker Daltonics). MALDI measurements were performed using a Smartbeam-II laser system (Bruker Daltonics) at a frequency of 500 Hz and 200 laser shots per scan. Different acquisition methods were used: two methods optimized for the detection of positive and negative ions in the *m/z*-range 2021.19–35,000, one for the detection of positive ions in the *m/z*-range 1010.65–8000, two for the detection of positive and negative ions in the *m/z*-range 796.71–7000. Collision-induced dissociation (CID) of carbohydrate fragment ions was performed on selected precursor ions in the *m/z*-range 91.89–8000. The collision energy was optimized for each precursor ion for efficient fragmentation.

2.7. Data analysis

Mass spectra were visually inspected using DataAnalysis 5.0 SR1 (Bruker Daltonics). Theoretical fragment ions of intact LLOs and O-PS fragments were generated in GlycoWorkbench 2.1 stable build 146 and Windows Excel 2002 (Damerell et al., 2012). Dispersity values were calculated using the peak intensity of intact LLOs in negative mode and

of B-type LLO fragments in positive mode (Stepto, 2009). The mass values used for this calculation were those of intact LLOs solely, in both negative and positive modes. Figures were made in Adobe Illustrator 2021.

3. Results and discussion

3.1. MALDI FT-ICR MS of extracted E. coli LLOs

The structural elucidation of glycoconjugates typically involves a combination of different analytical techniques. Mass spectrometry is well-suited for tackling complex samples requiring smaller amounts of material compared to other techniques like NMR spectroscopy. Among mass spectrometric methods, MALDI MS offers specific advantages such as straightforward analysis and data interpretation, broad mass detection range, wide dynamic concentration range, and minimal sample preparation needs. The generation of singly charged ions maximizes the mass difference between ions limiting the overlap between signals and simplifying the spectra. Previously, we showed the advantages of performing isotopic resolution measurements over a wide *m/z* range with MALDI FT-ICR MS for the characterization of proteins and polysaccharides (Nicolardi et al., 2015; Nicolardi et al., 2021). In this study, we analyzed O2-type LLOs by ultrahigh resolution MALDI FT-ICR MS in negative and positive ion modes (Fig. 2).

Deprotonated intact LLOs with a number of RUs ranging from 4 to 17 characterized the mass spectrum in negative ion mode while sodiated LLOs fragments with a number of RUs ranging from 5 to 15 and lacking the pyrophosphate-lipid moiety characterized the mass spectrum in positive mode. Such LLO fragments are derived from the cleavage between the phosphate and the glycan moiety resulting in glycan ions lacking one molecule of water (as in B_1-type fragment ions) (Domon & Costello, 1988). The dispersity (*Đ*) calculated from the observed O-antigen distribution was 1.075 ± 0.004 in negative mode and 1.035 ± 0.001 in positive mode (Stepto, 2009). The mass-average molar mass (*Mw*) and number-average molar mass (*Mn*) were 9270 ± 264 Da and 8623 ± 215 Da, respectively, in negative mode, and 9207 ± 128 Da and 8895 ± 117 Da in positive mode. Overall, these values are in good agreement with those obtained by LC-FLD-MS (used as an orthogonal method) for LLO-derived 2AB-labeled O2 polysaccharides from the same bacterial strain (Đ = 1.082; Mw = 9172 Da; Mn = 8477 Da; data not shown). The slightly higher Mw and Mn values and lower dispersity observed with MALDI may be attributed to factors such as ion transmission optimized for ions in the *m/z*-range 4000–12,000, differences in MALDI ionization efficiency, and quantification bias stemming from the decrease in resolving power across the *m/z* range.

Less abundant ion species were also detected in both ionization modes as exemplified for LLOs with 10 and 11 RUs in Fig. 3. A detailed examination of the mass spectra revealed the presence of LLO fragments in negative ion mode (Fig. 3a). Specifically, glycan-pyrophosphate and glycan-phosphate ion species lacking the lipid moiety were detected (e.g., species at *m/z* 9293.804 and *m/z* 9195.773). LLOs missing one FucNAc per chain were also observed (e.g., species at *m/z* 9026.952) indicating either a potential endogenous heterogeneity of the glycan moiety or an in-source fragmentation species. Additionally, LLO species lacking C_5H_8 were observed (e.g., species at *m/z* 9195.773) and identified as LLOs with shorter lipid moieties (i.e., C_{50} instead of C_{55}). This type of lipid heterogeneity was previously reported by Reid and coworkers, who identified shorter and longer forms of the undecaprenyl lipid (i.e., C_{45}, C_{50}, and C_{60}) in *Campylobacter jejuni* (Reid et al., 2009).

In positive ionization mode, intact LLOs were detected as minor species with either one or two hydrogen-to-sodium exchanges (e.g. *m/z* 9260.116 and *m/z* 9281.116, Fig. 3b). The relative intensity of LLOs missing one FucNAc per chain was more than double compared to detection in negative ion mode (i.e. the ratio O-PSs-1FucNAc/O-PSs was 0.06 ± 0.01 in negative mode and 0.13 ± 0.03 in positive mode). This higher value may indicate a contribution of in-source fragmentation to

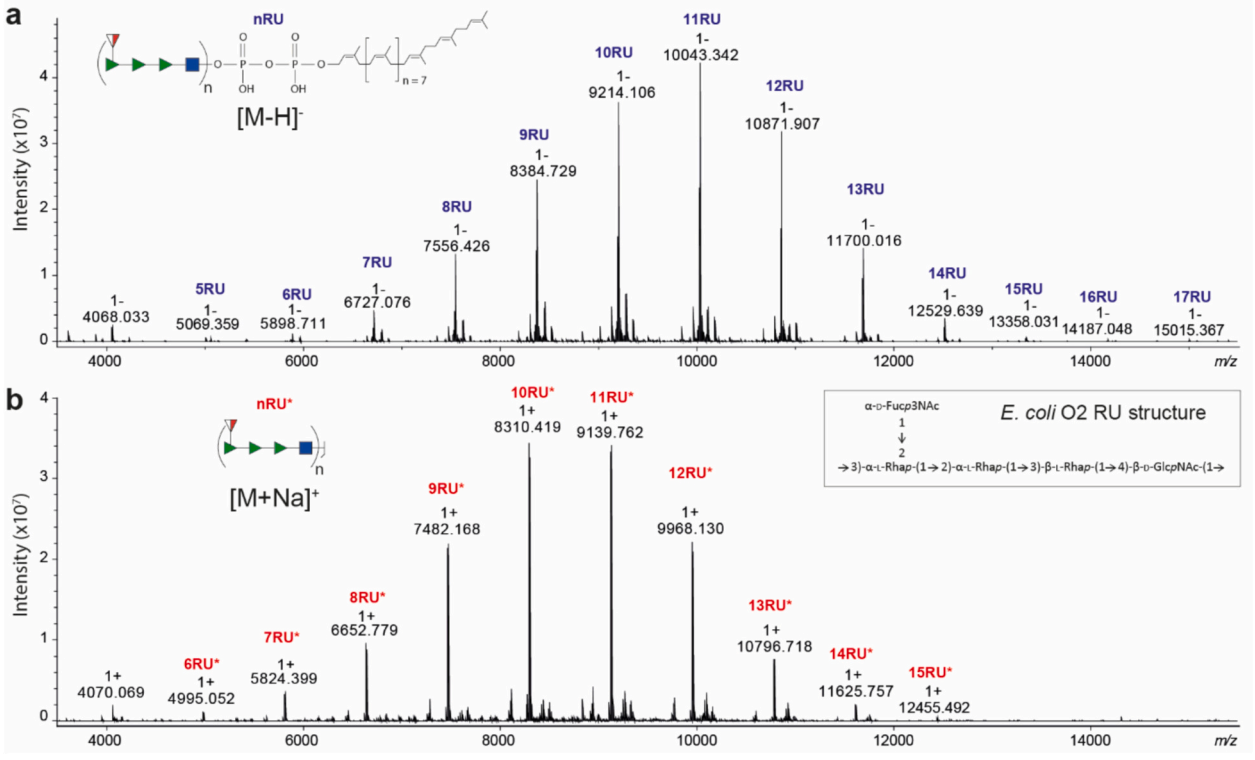

Fig. 2. MALDI FT-ICR mass spectra of *E. coli* O2 LLOs acquired in (**a**) negative and (**b**) positive ion mode. Deprotonated intact LLOs (blue labels) were detected in negative mode while sodiated B_1-type O-PSs fragments (red/asterisk labels) were detected in positive mode. The RU structure of *E. coli* O2 O-PSs is reported in the inset (Yang et al., 2018). SNFC symbols: rhamnose (Rha), green triangle; *N*-acetylglucosamine (GlcNAc), blue square; *N*-acetylfucosamine (FucNAc), white/red triangle.

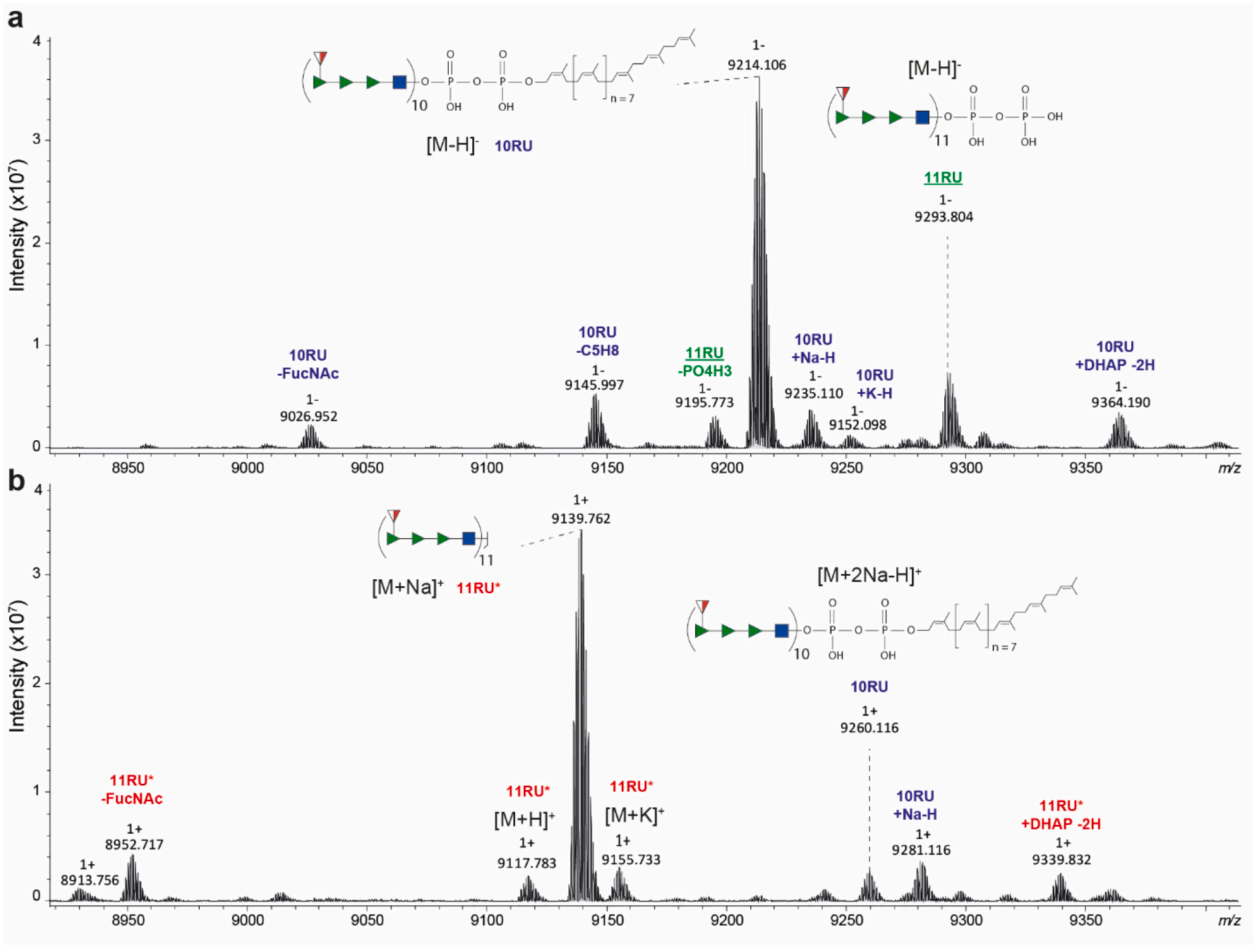

Fig. 3. Enlargement of the MALDI FT-ICR mass spectra of *E. coli* O2 LLOs acquired in (a) negative and (b) positive ion modes depicted in Fig. 2. Intact LLOs (blue labels) were the most abundant species in negative mode while fragmented LLOs missing the pyrophosphate-lipid moiety (red/asterisk labels) were predominant in positive mode. Fragmented LLOs missing the lipid moiety (green/underscored labels) were observed in negative mode. Heterogeneity of both the lipid and the glycan moieties was observed namely LLOs with a shorter lipid (i.e. peak at *m/z* 9145.997 in negative mode) and LLOs missing one FucNAc residue per chain (e.g. peak at *m/z* 8952.717 in positive mode). SNFC symbols: rhamnose (Rha), green triangle; *N*-acetylglucosamine (GlcNAc), blue square; *N*-acetylfucosamine (FucNAc), white/red triangle.

the formation of LLOs-FucNAc species from sodiated LLOs.

Measurements of LLOs at isotopic resolution enhance the confidence in identifying detected species. Such measurements are not exclusive to FT-ICR mass analyzers; modern MALDI TOF MS systems also achieve isotopic mass resolution at high *m/z* values (Klein et al., 2024). TOF MS provides constant resolving power across the entire *m/z* range, whereas the performance of FT-ICR MS improves at lower *m/z* values. For example, Klein and coworkers reported a constant resolving power of ~40,000 across a *m/z* range up to ~18,500 using a qTOF MS system. In comparison, our FT-ICR MS acquisition settings demonstrated resolving powers of 18,013 at *m/z* 15,015.367, 25,836 at *m/z* 10,043.342, and 51,159 at *m/z* 5069.3586. While FT-ICR MS can provide even higher resolving power with extended transient times, this comes at the cost of increased analysis time (Dilillo et al., 2017; Nicolardi et al., 2015).

The heterogeneity of *E. coli* O-antigens may be increased by the presence of non-sugar components such as amide-linked amino acids, and pyruvate, lactyl and acetyl groups with this latter being the most frequent modification observed on RUs (Liu et al., 2019). For example, the RU of O25B O-antigen contains an *O*-acetylated rhamnose residue (Szijártó et al., 2014). O-antigens may be further modified at the non-reducing end by end-capping groups such as methyl and phosphoglycerol groups (Clarke et al., 2004; Di Marco et al., 2024). Our analysis corroborated the absence of RU modifications or end-capping of the O2 LLOs, as in native LPS, confirming the success of the genetic editing process (Jansson et al., 1987).

The analyzed LLOs were purified from a crude extract using a reversed-phase solid-phase extraction cartridge. While this method successfully enriched the LLOs, it also co-purified other biomolecules. For instance, two unidentified intense species were detected in negative ion mode at *m/z* 3022.7264 and *m/z* 4066.0073 (**Fig. S1**). These species did not hinder the detection of the O2-type LLOs but could potentially interfere with the analysis of other O-type LLOs. For example, they might suppress the LLO signal if present at a higher concentration.

3.2. *Direct E. coli O-antigen analysis by MALDI FT-ICR MS from hydrolyzed biomass*

Recently, Urakami and Hinou have reported on a fast MALDI MS method for O-typing Gram-negative bacteria directly from single or multiple colonies of clinical strains (Urakami & Hinou, 2024; Urakami & Hinou, 2025). The method allows the detection of O-antigen fragments generated by mild acidic hydrolysis of LPS molecules on the surface of bacteria without the need for further purification. The key factor of the method is the use of a specific MALDI matrix mixture composed of sodium or potassium bicarbonate, DHB and 1,5-DAN. The presence of cations enhances the ionization of glycans while suppressing the ionization of other molecule types (Nicolardi et al., 2022; Urakami & Hinou, 2022). In this study, we investigated the applicability of this approach

for the analysis of *E. coli* O2 LLOs produced by a genetically modified precursor strain that only presents rough LPS on its surface (Fig. 1). The MALDI FT-ICR mass spectrum obtained from the hydrolyzed *E. coli* O2 biomass is reported in Fig. 4. Different hydrolyzed O-antigen fragments composed of intact RUs ranging from one up to four were detected (e.g. 1RU at *m/z* 869.3409 and 4RU at *m/z* 3354.3893, Fig. 4a), as well as glycan fragments derived from the hydrolysis of intra-RU glycosidic bonds (Fig. 4b). These latter O-antigen fragments provided additional structural insights that corroborated the RU composition; however, this also affected the determination of the original structural heterogeneity of O-PSs. For example, hydrolyzed O-antigen fragments missing one FucNAc residue (e.g., 2RUs-FucNAc at *m/z* 1510.5964) were detected at a much higher abundance (i.e. the ratio O-PSs-1FucNAc/O-PSs was 0.66 ± 0.45) compared to the analysis performed at intact LLOs level (see Fig. 3a). The mass spectrum was also enriched by the presence of low-intensity B-type ions (e.g., fragments at *m/z* 851.3290, *m/z* 1492.5827 and *m/z* 1679.6729) and cross-ring fragments (e.g., fragments at *m/z* 1596.6345) that generated from ISD fragmentation during the ionization process.

Our results demonstrate that Urakami and Hinou's method is effective for analyzing *E. coli* O2 O-PSs derived from an engineered *E. coli* strain. This strain does not display O-antigens on the surface-exposed LPS molecules of the external membrane but instead presents them solely as LLOs. However, the method does not yield quantitative insights into potential heterogeneity in the RU composition.

3.3. Structural characterization of O-antigen RU by MS/MS

In our previous study on the MALDI-ISD FT-ICR MS characterization of glycoconjugate vaccines carrying *E. coli* O-antigens, we showed that the monosaccharide composition of the RU could be confirmed by MS/MS analysis of B-type ions corresponding to 1RU and 2RUs (Nicolardi et al., 2022). In this study, we applied the same approach to characterize B-type ions and hydrolyzed O-antigen fragments generated from extracted LLOs and hydrolyzed biomass, respectively. The obtained fragmentation patterns confirmed the success of the bioengineering process and provided a fingerprint that can be used to corroborate the RU structure in glycoconjugate bacterial vaccines carrying the same type of O-antigen (Fig. 5). For example, the CID mass spectrum of a B-ion corresponding to 2RUs that was generated by MALDI-ISD MS of LLOs is reported in Fig. 5a. We compared this spectrum with the fragmentation pattern obtained from the same type of fragment ion that was generated from the MALDI-ISD MS analysis of a glycoconjugate carrying O2 O-PSs (Fig. 5b) showing a high similarity between the two spectra. Of note, MS/MS analysis of small intact LLO ions observed in negative mode was hampered by the low signal intensity of these species even at higher laser fluence.

The MS/MS analysis of hydrolyzed O-antigen fragments also provided valuable structural insights into the O2 O-PS RU. However, some differences were observed between the CID mass spectra obtained from hydrolyzed LLOs and those obtained from ISD fragments of the glycoconjugate vaccine (**Fig. S2**). In fact, despite differences in relative peak intensities, the cleavage patterns observed between the two types of ions were similar.

It must be noted that cross-ring fragment ions were detected at a very low signal intensity (see Fig. 5a) consequently, the analysis of the glycosidic linkages was not included in the study.

Given the structural variation between *E. coli* O-serotypes, these

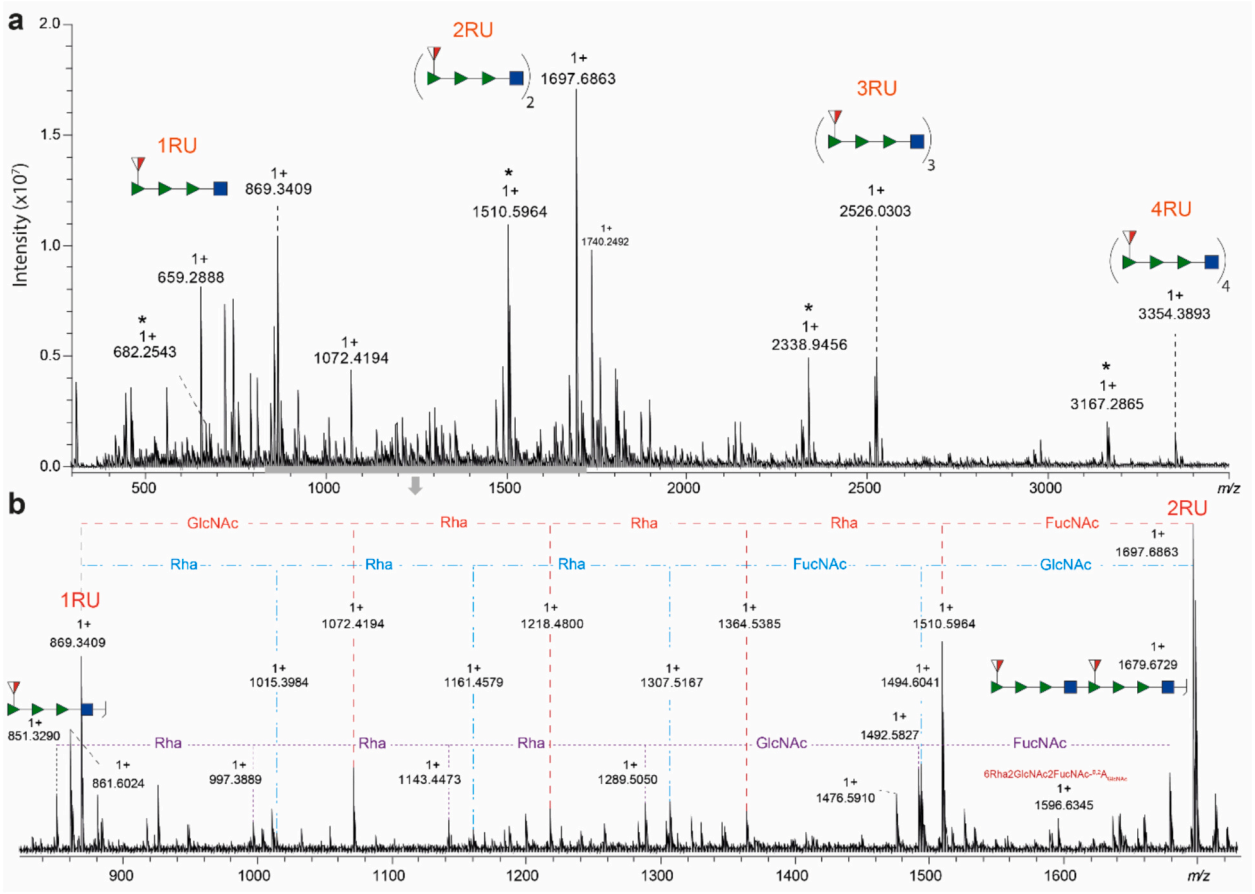

Fig. 4. MALDI FT-ICR mass spectrum of *E. coli* O2 biomass after mild acidic hydrolysis (**a**). Hydrolyzed O-antigen fragments composed of intact RUs were detected as well as fragments derived from intra-RU cleavages (see colored ladders) (**b**). * indicates nRU-FucNAc species. SNFC symbols: rhamnose (Rha), green triangle; *N*-acetylglucosamine (GlcNAc), blue square; *N*-acetylfucosamine (FucNAc), white/red triangle.

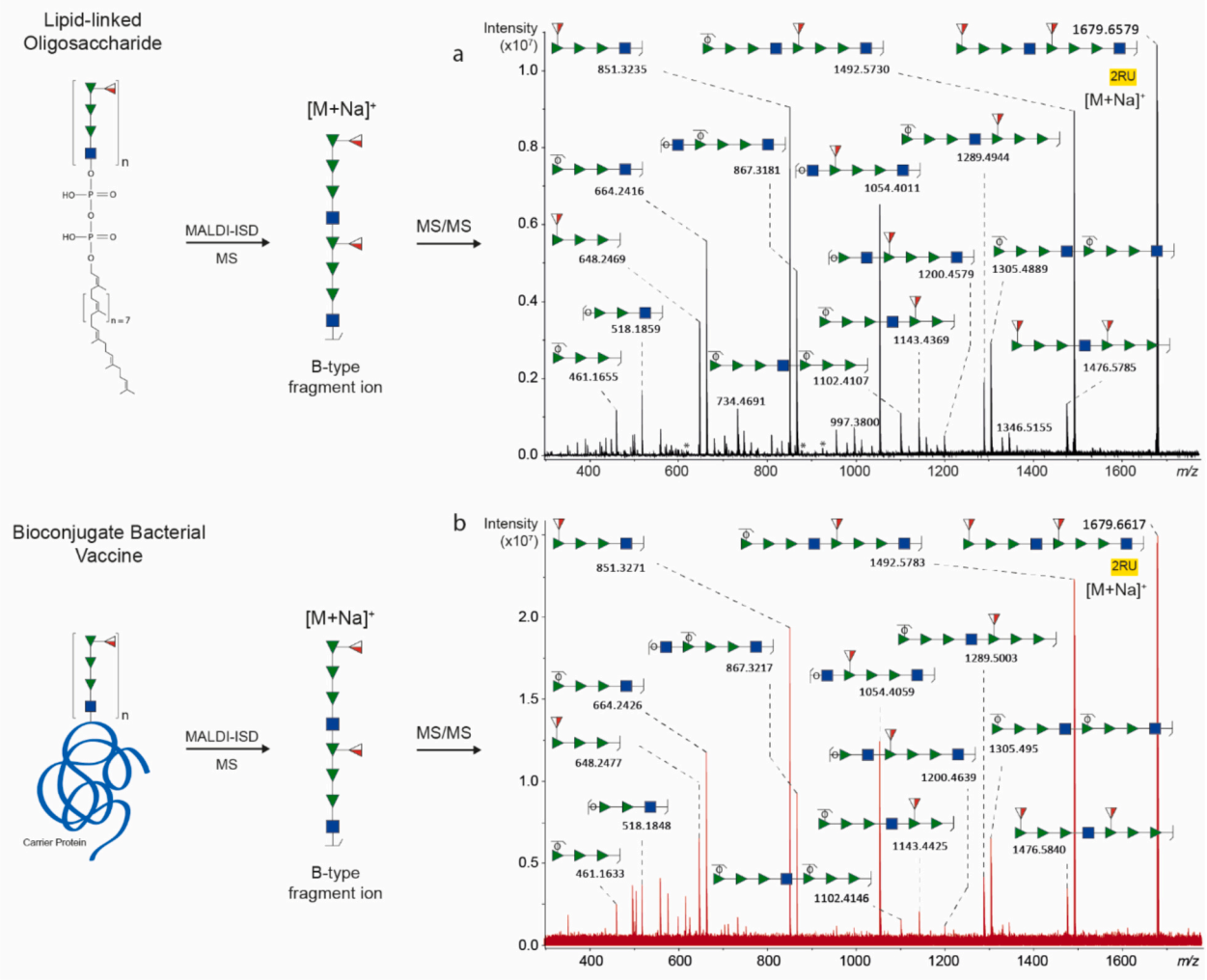

Fig. 5. MALDI-ISD CID FT-ICR mass spectra generated from B-type fragment ions corresponding to 2RUs from (**a**) *E. coli* O2 LLOs and (**b**) a glycoconjugate carrying *E. coli* O2 O-PSs (Figure modified from Nicolardi et al. Analytical Chemistry 2022, 94, 12, 4979–4987) (Nicolardi et al., 2022). These mass spectra support a structural consistency of O-PSs on the two types of biomolecules. SNFC symbols: rhamnose (Rha), green triangle; *N*-acetylglucosamine (GlcNAc), blue square; *N*-acetylfucosamine (FucNAc), white/red triangle. * cross-ring fragments detected at *m/z* 619.2322, *m/z* 879.3890 and *m/z* 925.3595.

characterization strategies may need adjustments for O-PSs with significantly different physicochemical properties or modifications. Nevertheless, isotopic resolution measurements by MALDI MS across a broad *m/z* range offer valuable structural insights that can complement other analytical techniques such as NMR spectroscopy supporting the development of glycoconjugate bacterial vaccines.

CRediT authorship contribution statement

Ieva Palubeckaite: Writing – review & editing, Writing – original draft, Methodology, Investigation, Formal analysis. **Alan B. Moran:** Writing – review & editing, Resources, Project administration, Conceptualization. **Dario A.T. Cramer:** Writing – review & editing, Investigation. **Anabel Torrente-López:** Writing – review & editing, Investigation. **Wiep Klaas Smits:** Writing – review & editing, Investigation. **Eveline Weerdenburg:** Writing – review & editing, Investigation, Conceptualization. **Ali Al Kaabi:** Writing – review & editing, Investigation, Conceptualization. **Michel Beurret:** Writing – review & editing, Project administration, Methodology, Investigation, Conceptualization. **Chakkumkal Anish:** Writing – review & editing, Project administration, Methodology, Investigation, Funding acquisition. **Manfred Wuhrer:** Writing – review & editing, Writing – original draft, Project administration, Methodology, Investigation, Funding acquisition, Conceptualization. **Simone Nicolardi:** Writing – review & editing, Writing – original draft, Supervision, Methodology, Formal analysis, Conceptualization.

Declaration of competing interest

The authors declare the following financial interests/personal relationships which may be considered as potential competing interests: Simone Nicolardi reports financial support was provided by Janssen Vaccines and Prevention BV. Ieva Palubeckaite reports financial support was provided by Janssen Vaccines and Prevention BV. Dario A. T. Cramer reports financial support was provided by Janssen Vaccines and Prevention BV. Anabel Torrente-Lopez reports financial support was provided by Janssen Vaccines and Prevention BV. Alan B. Moran reports a relationship with Janssen Vaccines and Prevention BV that includes: employment. Eveline Weerdenburg reports a relationship with Janssen Vaccines and Prevention BV that includes: employment. Michel Beurret reports a relationship with Janssen Vaccines and Prevention BV that includes: employment. Ali Al Kaabi reports a relationship with Janssen Vaccines and Prevention AG that includes: employment. Chakkumkal Anish reports a relationship with Janssen Vaccines and Prevention BV that includes: employment. The study stems from a service collaboration between Leiden University Medical Center and Janssen Vaccines &

Prevention B.V. This pharmaceutical company has been involved in the development of bioconjugate bacterial vaccines against *E. coli*.

If there are other authors, they declare that they have no known competing financial interests or personal relationships that could have appeared to influence the work reported in this paper.

Acknowledgment

This work was supported by Johnson & Johnson Innovative Medicine (Janssen Vaccines and Prevention B.V.). We thank Nienke Prins for contributing to *E. coli* culturing and bacterial biomass preparation.

Appendix A. Supplementary data

Supplementary data to this article can be found online at https://doi.org/10.1016/j.carbpol.2025.123928.

Data availability

Data will be made available on request.

References

Alley, W. R., Jr., Mann, B. F., & Novotny, M. V. (2013). High-sensitivity analytical approaches for the structural characterization of glycoproteins. *Chemical Reviews, 113*, 2668–2732.

Clarke, B. R., Cuthbertson, L., & Whitfield, C. (2004). Nonreducing terminal modifications determine the chain length of polymannose O antigens of Escherichia coli and couple chain termination to polymer export via an ATP-binding cassette transporter*. *Journal of Biological Chemistry, 279*, 35709–35718.

Damerell, D., Ceroni, A., Maass, K., Ranzinger, R., Dell, A., & Haslam, S. M. (2012). The GlycanBuilder and GlycoWorkbench glycoinformatics tools: Updates and new developments. *Biological Chemistry, 393*, 1357–1362.

Di Marco, F., et al. (2024). Comprehensive characterization of bacterial glycoconjugate vaccines by liquid chromatography - mass spectrometry. *Carbohydrate Polymers, 341*, Article 122327.

Dilillo, M., et al. (2017). Ultra-high mass resolution MALDI imaging mass spectrometry of proteins and metabolites in a mouse model of glioblastoma. *Scientific Reports, 7*, 603.

van den Dobbelsteen, G. P. J. M., et al. (2016). Immunogenicity and safety of a tetravalent E. Coli O-antigen bioconjugate vaccine in animal models. *Vaccine, 34*, 4152–4160.

Domon, B., & Costello, C. E. (1988). A systematic nomenclature for carbohydrate fragmentations in FAB-MS/MS spectra of glycoconjugates. *Glycoconjugate Journal, 5*, 397–409.

Dow, J. M., Mauri, M., Scott, T. A., & Wren, B. W. (2020). Improving protein glycan coupling technology (PGCT) for glycoconjugate vaccine production. *Expert Review of Vaccines, 19*, 507–527.

Feldman, M. F., et al. (2005). Engineering N-linked protein glycosylation with diverse O antigen lipopolysaccharide structures in Escherichia coli. *Proceedings of the National Academy of Sciences, 102*, 3016–3021.

Fierro, C. A., et al. (2023). Safety, Reactogenicity, immunogenicity, and dose selection of 10-valent Extraintestinal pathogenic Escherichia coli bioconjugate vaccine (VAC52416) in adults aged 60–85 years in a randomized, multicenter, interventional, first-in-human, phase 1/2a study. *Open Forum Infectious Diseases, 10*.

Fratamico, P. M., DebRoy, C., Liu, Y., Needleman, D. S., Baranzoni, G. M., & Feng, P. (2016). Advances in molecular serotyping and subtyping of Escherichia coli. *Frontiers in Microbiology, 7*, 644.

Frost, I., et al. (2023). The role of bacterial vaccines in the fight against antimicrobial resistance: An analysis of the preclinical and clinical development pipeline. *The Lancet Microbe, 4*, e113–e125.

Guo, H., et al. (2005). Molecular analysis of the O-antigen gene cluster of *Escherichia coli* O86:B7 and characterization of the chain length determinant gene (*wzz*). *Applied and Environmental Microbiology, 71*, 7995–8001.

Harvey, D. J. (2025). Analysis of carbohydrates and glycoconjugates by matrix-assisted laser desorption/ionization mass spectrometry: An update for 2021-2022. *Mass Spectrometry Reviews, 44*, 213–453.

Hernandez-Pastor, L., et al. (2023). Clinical burden of invasive Escherichia coli disease among older adult patients treated in hospitals in the United States. *BMC Infectious Diseases, 23*, 550.

Huttner, A., et al. (2017). Safety, immunogenicity, and preliminary clinical efficacy of a vaccine against extraintestinal pathogenic Escherichia coli in women with a history of recurrent urinary tract infection: A randomised, single-blind, placebo-controlled phase 1b trial. *The Lancet Infectious Diseases, 17*, 528–537.

Ikuta, K. S., et al. (2022). Global mortality associated with 33 bacterial pathogens in 2019: A systematic analysis for the global burden of disease study 2019. *The Lancet, 400*, 2221–2248.

Jansson, P.-E., Lennholm, H., Lindberg, B., Lindquist, U., & Svenson, S. B. (1987). Structural studies of the O-specific side-chains of the Escherichia coli O2 lipopolysaccharide. *Carbohydrate Research, 161*, 273–279.

Kaper, J. B., Nataro, J. P., & Mobley, H. L. T. (2004). Pathogenic Escherichia coli. *Nature Reviews Microbiology, 2*, 123–140.

Khlebnikov, A., Risa, Ø., Skaug, T., Carrier, T. A., & Keasling, J. D. (2000). Regulatable arabinose-inducible gene expression system with consistent control in all cells of a culture. *Journal of Bacteriology, 182*, 7029–7034.

Klein, D. R., Rivera, E. S., Caprioli, R. M., & Spraggins, J. M. (2024). Imaging mass spectrometry of isotopically resolved intact proteins on a trapped ion-mobility quadrupole time-of-flight mass spectrometer. *Analytical Chemistry, 96*, 5065–5070.

Kowarik, M., et al. (2021). The development and characterization of an E. Coli O25B bioconjugate vaccine. *Glycoconjugate Journal, 38*, 421–435.

Liu, B., et al. (2019). Structure and genetics of Escherichia coli O antigens. *FEMS Microbiology Reviews, 44*, 655–683.

MacKinnon, M. C., et al. (2021). Increasing incidence and antimicrobial resistance in Escherichia coli bloodstream infections: A multinational population-based cohort study. *Antimicrobial Resistance & Infection Control, 10*, 131.

Manges, A. R., Geum, H. M., Guo, A., Edens, T. J., Fibke, C. D., & Pitout, J. D. D. (2019). Global Extraintestinal pathogenic Escherichia coli (ExPEC) lineages. *Clinical Microbiology Reviews, 32*. https://doi.org/10.1128/cmr.00135-00118

del Mar Tavío, M., Vila, J., Jm, R., Ruiz, J., Martín-Sánchez, A. M., & de Anta MaT, J. (2000). Resolution of high-molecular-weight components in lipopolysaccharides of Escherichia coli, Morganella morganii, Citrobacter freundii and Citrobacter diversus strains with sodium dodecyl sulfate polyacrylamide gels. *Journal of Microbiological Methods, 39*, 145–148.

Naghavi, M., et al. (2024). Global burden of bacterial antimicrobial resistance 1990-2021: A systematic analysis with forecasts to 2050. *The Lancet, 404*, 1199–1226.

Nicolardi, S., Switzar, L., Deelder, A. M., Palmblad, M., & van der Burgt, Y. E. M. (2015). Top-down MALDI-in-source decay-FTICR mass spectrometry of isotopically resolved proteins. *Analytical Chemistry, 87*, 3429–3437.

Nicolardi, S., et al. (2021). Analysis of synthetic monodisperse polysaccharides by wide mass range ultrahigh-resolution MALDI mass spectrometry. *Analytical Chemistry, 93*, 4666–4675.

Nicolardi, S., et al. (2022). Glycan and protein analysis of Glycoengineered Bacterial E. Coli vaccines by MALDI-in-source decay FT-ICR mass spectrometry. *Analytical Chemistry, 94*, 4979–4987.

Perry, M. B., MacLean, L., & Griffith, D. W. (1986). Structure of the O-chain polysaccharide of the phenol-phase soluble lipopolysaccharide of Escherichia coli 0: 157:H7. *Biochemistry and Cell Biology, 64*, 21–28.

Poolman, J. T., & Wacker, M. (2015). Extraintestinal pathogenic Escherichia coli, a common human pathogen: Challenges for vaccine development and Progress in the field. *The Journal of Infectious Diseases, 213*, 6–13.

Pupo, E., van der Ley, P., & Meiring, H. D. (2021). Nanoflow LC–MS method allowing in-depth characterization of natural heterogeneity of complex bacterial lipopolysaccharides. *Analytical Chemistry, 93*, 15832–15839.

Qiu, L., et al. (2024). Vaccines against extraintestinal pathogenic Escherichia coli (ExPEC): Progress and challenges. *Gut Microbes, 16*, 2359691.

Raetz, C. R. H., & Whitfield, C. (2002). Lipopolysaccharide endotoxins. *Annual Review of Biochemistry, 71*, 635–700.

Reeves, P. (1995). Role of O-antigen variation in the immune response. *Trends in Microbiology, 3*, 381–386.

Reid, C. W., Stupak, J., Chen, M. M., Imperiali, B., Li, J., & Szymanski, C. M. (2008). Affinity-capture tandem mass spectrometric characterization of Polyprenyl-linked oligosaccharides: Tool to study protein N-glycosylation pathways. *Analytical Chemistry, 80*, 5468–5475.

Reid, C. W., Stupak, J., Szymanski, C. M., & Li, J. (2009). Analysis of bacterial lipid-linked oligosaccharide intermediates using porous graphitic carbon liquid chromatography-electrospray ionization mass spectrometry: Heterogeneity in the Polyisoprenyl Carrier revealed. *Analytical Chemistry, 81*, 8472–8478.

Reid, C. W., Stupak, J., & Szymanski, C. M. (2010). Characterization of lipid-linked oligosaccharides by mass spectrometry. *Methods in Molecular Biology, 600*, 187–197.

Stepto, R. F. T. (2009). Dispersity in polymer science (IUPAC recommendations 2009). *Pure and Applied Chemistry, 81*, 351–353.

Szijártó, V., Lukasiewicz, J., Gozdziewicz, T. K., Magyarics, Z., Nagy, E., & Nagy, G. (2014). Diagnostic potential of monoclonal antibodies specific to the unique O-antigen of multidrug-resistant epidemic Escherichia coli clone ST131-O25b:H4. *Clinical and Vaccine Immunology, 21*, 930–939.

Tirsoaga, A., et al. (2007). Simple method for Repurification of endotoxins for biological use. *Applied and Environmental Microbiology, 73*, 1803–1808.

Urakami, S., & Hinou, H. (2022). Glycan-selective MALDI in-source decay analysis of intact glycoproteins. *Analysis & Sensing, 2*, Article e202100040.

Urakami, S., & Hinou, H. (2024). MALDI glycotyping of O-antigens from a single colony of gram-negative bacteria. *Scientific Reports, 14*, 12719.

Urakami, S., & Hinou, H. (2025). MALDI O-antigen glycotyping of Y. pseudotuberculosis using DAN/DHB/K matrix. *BBA. Advances, 7*, Article 100131.

Wang, J., Qin, C., Xu, Y., Yin, J., Hu, J., & Guo, X. (2023). Structural and genetic identification of the O-antigen from an Escherichia coli isolate, SD2019180, representing a novel serogroup. *International Journal of Molecular Sciences, 24*, 15040.

Wantuch, P. L., et al. (2024). Heptavalent O-antigen bioconjugate vaccine exhibiting differential functional antibody responses against diverse Klebsiella pneumoniae isolates. *The Journal of Infectious Diseases, 230*, 578–589.

Weerdenburg, E., et al. (2022). Global distribution of O serotypes and antibiotic resistance in Extraintestinal pathogenic Escherichia coli collected from the blood of

patients with bacteremia across multiple surveillance studies. *Clinical Infectious Diseases, 76*, e1236–e1243.
Wetter, M., Kowarik, M., Steffen, M., Carranza, P., Corradin, G., & Wacker, M. (2013). Engineering, conjugation, and immunogenicity assessment of Escherichia coli O121 O antigen for its potential use as a typhoid vaccine component. *Glycoconjugate Journal, 30*, 511–522.
Whitfield, C., Williams, D. M., & Kelly, S. D. (2020). Lipopolysaccharide O-antigens—Bacterial glycans made to measure. *Journal of Biological Chemistry, 295*, 10593–10609.
Woodward, R., et al. (2010). In vitro bacterial polysaccharide biosynthesis: Defining the functions of Wzy and Wzz. *Nature Chemical Biology, 6*, 418–423.
Yang, B., et al. (2018). Structural and genetic relatedness of the O-antigens of Escherichia coli O50 and O2. *Carbohydrate Research, 464*, 8–11.